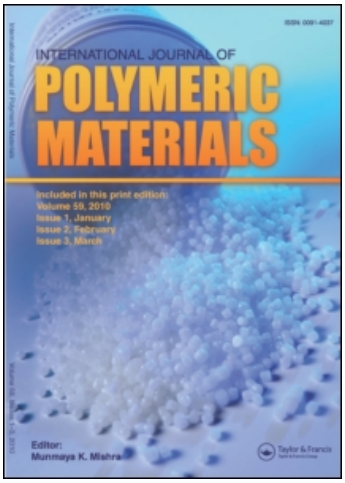

International Journal of Polymeric Materials
Publication details, including instructions for authors and subscription information:
http://www.informaworld.com/smpp/title~content=t713647664

Physical and Mechanical Behavior of Polymer Glasses. VI. the Role of Free Volume

M. S. Arzhakov[a]; S. A. Arzhakov[a]; Z. K. Suptel[b]; I. B. Kevdina[b]; V. P. Shantarovich[b]
[a] Polymer Department, Faculty of Chemistry, Moscow State University, Moscow, Russia [b] Semenov Institute of Chemical Physics, Russian Academy of Sciences, Moscow, Russia

To cite this Article Arzhakov, M. S. , Arzhakov, S. A. , Suptel, Z. K. , Kevdina, I. B. and Shantarovich, V. P.(2000) 'Physical and Mechanical Behavior of Polymer Glasses. VI. the Role of Free Volume', International Journal of Polymeric Materials, 47: 2, 169 — 194
To link to this Article: DOI: 10.1080/00914030008035059
URL: http://dx.doi.org/10.1080/00914030008035059

Intern. J. Polymeric Mater., 2000, Vol. 47, pp. 169–194
Reprints available directly from the publisher
Photocopying permitted by license only

Physical and Mechanical Behavior of Polymer Glasses. VI. the Role of Free Volume

M. S. ARZHAKOV [a,*], S. A. ARZHAKOV [a], Z. K. SUPTEL [b], I. B. KEVDINA [b] and V. P. SHANTAROVICH [b]

[a] *Polymer Department, Faculty of Chemistry, Moscow State University, Vorob'evy gory, Moscow, 119899 Russia;* [b] *Semenov Institute of Chemical Physics, Russian Academy of Sciences, ul. Kosygina, 4, Moscow, 117977 Russia*

(Received 5 January 1999)

For various polymer glasses, the temperature-induced recovery of residual deformation was studied. The ratio between the low-temperature and high-temperature recovery components is controlled by the difference between deformation temperature and glass transition temperature T_g of polymer samples independently of their chemical structure. This ratio correlates with polymer macroscopic mechanical characteristics such as elastic modulus and yield stress. Experimental results were treated in terms of the dynamics of segmental mobility within different structural sublevels with different packing densities. To correlate this mechanical response with the structural state of glassy polymers, positron annihilation lifetime spectroscopy (PALS) was used. For different polymer glasses, the microscopic segmental mobility and resultant macroscopic mechanical properties were shown to be controlled only by the development of the adequate free volume content which depends on the difference between testing temperature and T_g. These results allowed us to propose the general correlation between microstructure, microscopic molecular mobility, and macroscopic mechanical behavior of polymer glasses.

Keywords: Glassy polymers; mechanics; relaxation; structure; PALS

INTRODUCTION

Finding the correlation between microstructure and macroscopic mechanical behavior of amorphous glassy polymers seems to be rather

*Corresponding author.

difficult because no efficient experimental methods to study their structure are available. In many cases, the advances in this fundamental area are provided by examination of their physical and mechanical behavior. Studies in the temperature-induced recovery of residual deformation were shown [1–6] to be a very powerful experimental approach to provide an important information concerning the mechanism of deformation of glassy polymers.

In deformed polymer glasses, the temperature-induced recovery of residual deformation is known [1, 2] to involve the low-temperature component at temperatures well below glass transition temperature T_g (ε_1) and high-temperature component in the vicinity of T_g (ε_2) (Fig. 1). Note that the ratio between these two components depends on the strain (Fig. 2).

Low-temperature component ε_1 is accumulated in polymer samples during deformation to strains close to yield strain ε_y (Fig. 2, curve 2).

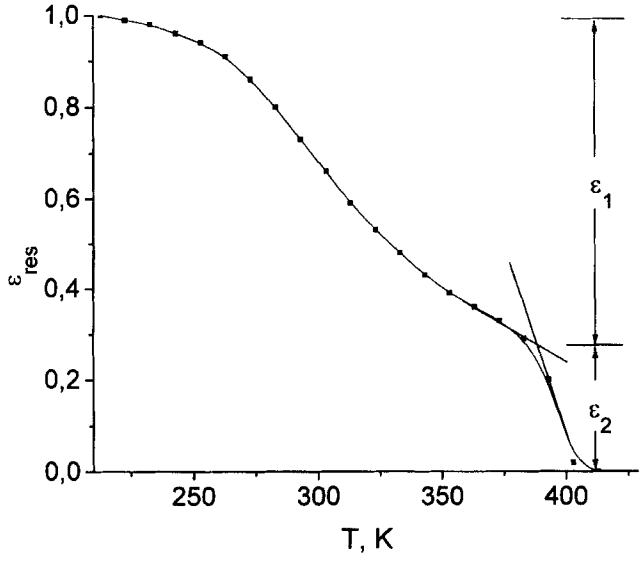

FIGURE 1 A typical temperature dependence of the relative residual deformation ε_{res}. (PMMA sample was uniaxially compressed to strain 20% at 293 K, cooled down in the stressed state with liquid nitrogen, released at this temperature, and heated with the heating rate of 0.8 k/min) [2].

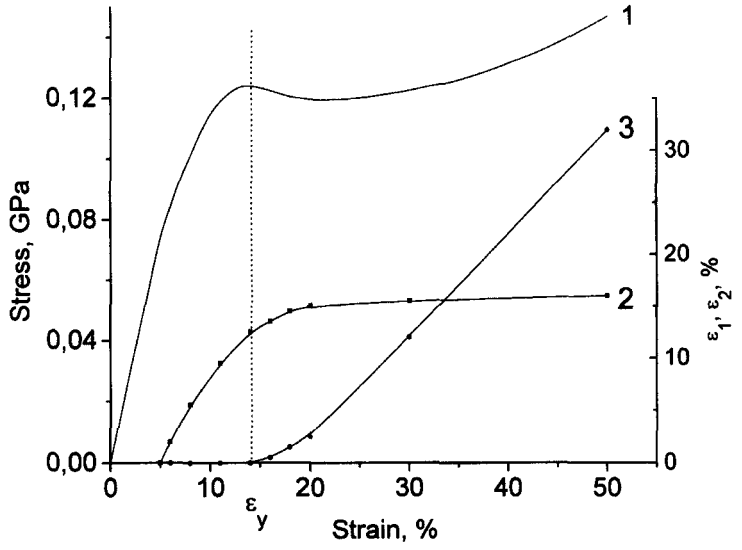

FIGURE 2 The stress-strain curve corresponding to the iniaxial compression of PMMA sample at 293 K (1) and low-temperature ε_1 (2) and high-temperature ε_2 components (3) of the temperature-induced recovery of residual deformation *versus* strain ε [2].

As strain exceeds the yield strain ε_y, the low-temperature component ε_1 shows no increase whereas the appearance and increase in the high-temperature component ε_2 are observed (Fig. 2, curve 3). The existence of the above two recovery components in the deformed polymer samples reveals the existence of the two corresponding deformation modes. From this standpoint, studying temperature-induced recovery of the residual deformation allows a correct identification of these deformation components.

The origin of the two-stage character of the temperature-induced recovery of residual deformation was analyzed from both experimental and theoretical viewpoints, and various theories for the deformation mechanism of glassy polymers were advanced.

When the structural model treats a glassy polymer as a homogeneous material with some density fluctuations, the mechanism of deformation involves the nucleation of small-scale plastic shear transformations [6, 7] or shear microdomains [8–10] and their further

degradation *via* transition into excited chain conformations. For the unloaded polymer sample, the low-temperature recovery of the macroscopic residual deformation is controlled by the local recovery of plastic shear transformations *via* transition to their initial state. The high-temperature recovery component is provided by the entropy recovery of the excited conformations of macromolecular coils *via* segmental mobility.

In the recent decades, the problems related to the structure of polymer glasses were widely discussed in literature, for example, in [11–17]. Polymer glasses are characterized by the structural inhomogeneity related to the existence of the heterogeneous ordered regions with an increased packing density (domains, clusters), and these regions are joined by tie-chains. These tie-chains constitute structural regions with lowered packing density. In other words, the structure of a glassy polymer may be presented as a set of structural sublevels with different packing densities. On the basis of this structural model, we advanced [5] the structural pattern of the deformation of glassy polymers when the deformation is presented as a gradual activation of segmental mobility within different structural sublevels.

In this work, for more detailed description of the molecular mechanism of glassy polymers deformation, the variations in the ratio between the low-temperature and high-temperature components of the temperature-induced recovery were studied by varying experimental regimes of deformation as well as by physicochemical modification. To establish the correlation between mechanical behavior and microstructural changes in initial polymers, mechanical tests were coupled with positron annihilation lifetime spectroscopy (PALS).

PALS is widely used to study the microstructure of polymers [16, 18–28]. Combination of PALS and mechanical tests was shown to be a very promising tool for studying the relationship between the structure and mechanical properties of glassy polymers. This experimental approach allowed one to follow the structural changes in polymers induced by plastic deformation and structural relaxation [18, 19, 22], to study the effect of microstructure of polymer glasses on the macroscopic mechanical response [23, 24], and to investigate the mechanical behavior of glassy polymer as a function of the structural changes associated with the introduction of low-molecular-mass additives [16].

EXPERIMENTAL

Preparation of Test Samples

In this work, we studied poly(methyl methacrylate) (PMMA), PMMA plasticized with dibutyl phthalate (DBPh) and diethyl siloxane oligomer (DES) containing 5 repeated units, poly(butyl methacrylate) (PBMA), polystyrene (PS), and random copolymers of methyl methacrylate (MMA) with butyl methacrylate (BMA), octyl methacrylate (OMA), and lauryl methacrylate (LMA).

Prior to polymerization and copolymerization, monomers were distilled in vacuum under nitrogen flow. Benzoyl peroxide (BP) and lauroyl peroxide (LP) were used as initiators of polymerization and copolymerization. BP and LP were purified by recrystallization from ethanol.

For homopolymers and copolymers, the monomer feed compositions were the following:

MMA/DBPh – 95/5, 90/10, and 80/20 (weight ratio), initiator – BP;
MMA/DES – 99.9/0.1, 99.5/0.5, and 98.7/1.3 (weight ratio), initiator – BP;
MMA/BMA – 100/0, 80/20, 70/30, 50/50, 0/100 (mole ratio), initiator – LP;
MMA/OMA – 95/5, 90/10, and 80/20, (mole ratio), initiator – LP;
MMA/LMA – 95/5, 90/10, and 85/15 (mole ratio), initiator – LP;
Styrene, initiator – BP.

For all mixtures, the content of initiator was 5×10^{-3} mol/l. Monomer mixtures were deoxygenated by a repeated freezing-defreezing procedure at a pressure of 10^{-2} mm Hg.

Polymerization and copolymerization were carried out in the sealed glass tubes with a diameter of 10 mm and a height of 100 mm at 333 K under vacuum. At the final stage of polymerization, to achieve a complete conversion, the temperature was increased up to temperatures above glass transition temperature of the corresponding polymer by 10 – 15 K.

Physical and Mechanical Characterization

Glass transition temperatures of the test samples were estimated by differential scanning calorimetry using a "Mettler TA-4000" thermal analyzer; heating rate was 20 K/min.

For the mechanical tests, the test samples were cut as cylinders with a height of 5 mm and a diameter of 5 mm. Prior to tests, the samples were annealed at temperatures above glass transition temperature by 10–15 K. Then, the samples were slowly cooled down to room temperature. The height of the as-prepared samples was denoted as h_0.

The test samples were uniaxially compressed at temperatures varying from 293 to 393 K. Strain rates were 1.7×10^{-5}, 1.7×10^{-4}, 1.7×10^{-3}, and $1.7 \times 10^{-2}\,s^{-1}$. The tests were performed using an UTS-10 tensile machine (Germany). Elastic modulus was estimated from the slope of the initial portion of $\sigma-\varepsilon$ curve at strains not above than 3%. The accuracy of estimation of elastic modulus E_0 and yield stress σ_y was equal to $\pm 5\%$. The height of the stressed samples was denoted as h_{def}. Then, the samples were unloaded at 293 K. Unloading rates were the same as loading rates.

To evaluate the ratio between low-temperature (ε_1) and high-temperature components (ε_2), temperature-induced relaxation of residual deformation was studied by measuring the changes in the height of the test samples on their heating in the temperature range from 293 K to T_g. At a certain temperature within this temperature interval, free-standing samples were allowed to relax for 30 min. The height of as-relaxed sample at a given temperature was denoted as h_T. Residual deformation at a given temperature was estimated as $\varepsilon_{res} = (h_0-h_T)/(h_0-h_{def})$ with an accuracy of $\pm 2\%$.

Note that the ratio $\varepsilon_1/\varepsilon_2$ or the contribution from ε_1 to the total relaxation of residual deformation $\varepsilon_1/(\varepsilon_1+\varepsilon_2)$ depends on the ratio between the applied strain and yield strain ε_y (Fig. 2, curves 2 and 3). In this work, for correct evaluation of $\varepsilon_1/(\varepsilon_1+\varepsilon_2)$, the samples were deformed to a relative strain $\varepsilon(\%) = \varepsilon_y(\%)+8$.

For all polymer samples, the parameters of the deformation and mechanical characteristics are summarized in Table I.

Characterization of Polymer Structure by PALS

Positron annihilation lifetime spectroscopy (PALS) was shown to provide an important information concerning the microstructure of polymers [16, 18–28]. In the early studies [19, 29–31], the time distributions of annihilation parameters showed that a marked fraction of both positrons and positronium (electron-positron system)

TABLE I Conditions of the deformation and the physical and mechanical characteristics of polymer samples

N	*Sample*	T_g, K	T_{def}, K	$\Delta T_{def}, K$	V_{def}, s^{-1}	ε_y,%	ε,%	σ_y, GPa	$\varepsilon_1/(\varepsilon_1+\varepsilon_2)$	E_0, GPa
1	PMMA	393	293	100	1.7×10^{-4}	12	20	0.124	0.88	1.50
			320	73	–	12	20	0.082	0.78	1.25
			333	60	–	10	18	0.071	0.73	1.03
			343	50	–	10	18	0.059	0.70	0.90
			353	40	–	7	15	0.051	0.61	0.80
			393	0	–		20	0	0	0.40
2	PMMA	393	293	100	1.7×10^{-2}	14	22	0.15	0.93	2.00
			–	–	1.7×10^{-3}	14	22	0.14	0.91	1.67
			–	–	1.7×10^{-4}	12	20	0.124	0.88	1.53
			–	–	1.7×10^{-5}	12	20	0.115	0.85	1.40
3	PMMA with									
	5 wt%	383	293	90	1.7×10^{-4}	11	19	0.102	0.85	1.45
	10 wt%	373	–	80	–	9	17	0.086	0.81	1.30
	20 wt% of DBPh	343	–	50	–	7	15	0.065	0.68	0.95
4	PMMA with									
	0.1 wt%	393	293	100	1.7×10^{-4}	12	20	0.135	0.93	1.75
	0.5 wt%	–	–	–	–	12	20	0.124	0.88	1.53
	1.3 wt% of DES	–	–	–	–	12	20	0.105	0.83	1.30
5	PS	363	293	70	1.7×10^{-2}	10	18	0.112	0.89	1.70
			–	–	1.7×10^{-3}	8	16	0.095	0.84	1.57
			–	–	1.7×10^{-4}	8	16	0.076	0.79	1.50
			–	–	1.7×10^{-5}	7	15	0.063	0.71	1.35
6	PBMA	293	293	0	1.7×10^{-4}		20	0	0	

TABLE I (Continued)

N	Sample	T_g, K	T_{def}, K	$\Delta T_{def}, K$	V_{def}, s^{-1}	ε_y,%	ε,%	σ_y, GPa	$\varepsilon_1/(\varepsilon_1+\varepsilon_2)$	E_0, GPa
7	(MMA	363	293	70	1.7×10^{-2}	12	20	0.119	0.89	1.80
	-*co*-BMA)		–	–	1.7×10^{-3}	12	20	0.104	0.86	1.79
	80/20		–	–	1.7×10^{-4}	10	18	0.084	0.79	1.43
			–	–	1.7×10^{-5}	10	18	0.064	0.72	1.30
8	(MMA	353	293	60	1.7×10^{-2}	12	20	0.107	0.87	1.75
	-*co*-		–	–	1.7×10^{-3}	12	20	0.082	0.82	1.65
	BMA)		–	–	1.7×10^{-4}	10	18	0.065	0.75	1.40
	70/30		–	–	1.7×10^{-5}	10	18	0.054	0.66	1.25
9	(MMA	333	293	40	1.7×10^{-2}	11	19	0.085	0.82	1.20
	-*co*-		–	–	1.7×10^{-3}	10	18	0.070	0.75	1.10
	BMA)		–	–	1.7×10^{-4}	8	16	0.059	0.62	0.90
	50/50		–	–	1.7×10^{-5}	8	16	0.045	0.49	0.75
10	(MMA	378	293	85	1.7×10^{-2}	12	20	0.133	0.92	1.55
	-*co*-		–	–	1.7×10^{-3}	12	20	0.110	0.87	1.45
	OMA)		–	–	1.7×10^{-4}	12	20	0.096	0.83	1.25
	95/5		–	–	1.7×10^{-5}	12	20	0.078	0.78	1.10
11	(MMA	363	293	70	1.7×10^{-2}	12	20	0.112	0.92	1.60
	-*co*-		–	–	1.7×10^{-3}	12	20	0.094	0.86	1.35
	OMA)		–	–	1.7×10^{-4}	10	18	0.077	0.80	1.10
	90/10		–	–	1.7×10^{-5}	10	18	0.060	0.70	1.05
12	(MMA	343	293	50	1.7×10^{-2}	11	19	0.086	0.87	1.50
	-*co*-		–	–	1.7×10^{-3}	11	19	0.067	0.80	1.25
	OMA)		–	–	1.7×10^{-4}	8	16	0.055	0.71	1.10
	80/20		–	–	1.7×10^{-5}	8	16	0.035	0.59	0.90
13	(MMA	368	293	75	1.7×10^{-2}	12	20	0.110	0.91	1.75
	-*co*-		–	–	1.7×10^{-3}	12	20	0.105	0.86	1.65
	LMA)		–	–	1.7×10^{-4}	11	19	0.089	0.81	1.45
	95/5		–	–	1.7×10^{-5}	11	19	0.080	0.76	1.30

14	(MMA	353	293	60	1.7×10^{-2}	12	20	0.091	0.87	1.65
	-co-		–	–	1.7×10^{-3}	11	19	0.075	0.84	1.53
	LMA)		–	–	1.7×10^{-4}	9	17	0.060	0.75	1.41
	90/10		–	–	1.7×10^{-5}	9	17	0.040	0.66	1.20
15	(MMA	338	293	45	1.7×10^{-2}	9	17	0.082	0.83	1.47
	-co-		–	–	1.7×10^{-3}	8	16	0.063	0.77	1.25
	LMA)		–	–	1.7×10^{-4}	6	14	0.050	0.67	0.95
	85/15		–	–	1.7×10^{-5}	6	14	0.043	0.53	0.85

annihilate after their localization in the free volume microregions (holes).

Numerous model experiments [30, 32, 33] allowed one to conclude that, in the heterogeneous structures, the positrons tend to localize and annihilate in the free volume holes within the ordered structural regions, whereas the positronium occupies and annihilates in the free volume holes within the disordered structural regions [19]. These theoretical speculations were supported by the PAL studies of heterogeneous polymer materials such as semicrystalline polymers [22], polymers containing rigid inorganic fillers [19, 22], and cured epoxy polymers [28].

According to the heterogeneous structural model of a glassy polymer [11 – 17], the positrons are expected to occupy and annihilate in the structural sublevels with increased packing densities, whereas positronium – in the structural sublevels with lowered packing densities.

For the three-component analysis, the shortest-lived component with lifetime τ_1 and intensity I_1 is associated with the annihilation of singlet positronium (^{1}Ps) and non-localized positrons. The component with lifetime τ_2 and intensity I_2 is partially associated with the non-localized positrons and is primarily related to a preferential localization of the positrons in the free volume microregions in the structural sublevels with increased packing densities. Orthopositronium occupies and annihilates in free volume microregions in structural sublevels with lowered packing densities, and this factor contributes to the longest-lived component with the lifetime τ_3 and intensity I_3. Parameters τ_i and I_i are associated with effective size and concentration of free volume microregions in structural sublevels with increased packing densities ($i = 2$) and lowered packing densities ($i = 3$). However, in this work, we considered only the changes in τ_i and I_i values to estimate qualitatively the changes in free volume as a result of physicochemical modification of polymer samples.

PAL measurements were carried out at 293 K using a conventional ORTEC spectrometer with a time-resolution (full width on a half maximum of the prompt coincidence curve) of 230 ps. ^{22}Na sandwiched between the two sheets of nickel foil was used as a positron source. For both three-component and four-component analysis, PATFIT computing program [34] was used to calculate the annihilation characteristics (lifetimes τ_i and intensities I_i) from the corresponding lifetime

distribution of annihilation radiation. A continuos analysis of the PAL spectra was performed using CONTIN program [35–38].

RESULTS AND DISCUSSION

For the polymer samples compressed at different strain rates, Figure 3 (A) shows the contribution from the low-temperature component to total residual deformation $\varepsilon_1/(\varepsilon_1+\varepsilon_2)$ *versus* the relative temperature of deformation $\Delta T_{def} = T_g - T_{def}$. At each strain rate, all experimental data fit one curve, and as ΔT_{def} is decreased, $\varepsilon_1/(\varepsilon_1+\varepsilon_2)$ decreases. This trend is independent of the variations in ΔT_{def}: increasing T_{def} at a fixed T_g (PMMA samples) or decreasing T_g at a fixed T_{def} (plasticized PMMA and copolymer samples). When T_{def} approaches $T_g(\Delta T_{def} \rightarrow 0)$, the recovery of residual deformation is controlled only by the

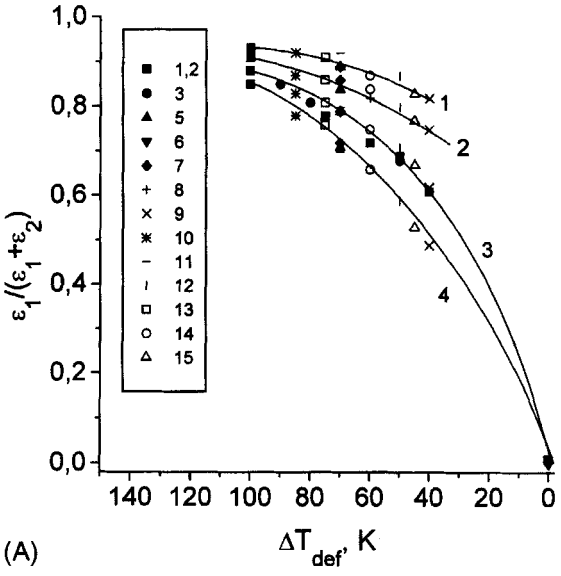

FIGURE 3 The contribution from the low-temperature component to the total temperature-induced recovery of residual deformation $\varepsilon_1/(\varepsilon_1+\varepsilon_2)$ *versus* the relative deformation temperature ΔT_{def} for the polymer samples compressed with the strain rates 1.7×10^{-2} (1), 1.7×10^{-3} (2), 1.7×10^{-4} (3), and $1.7\times10^{-5}\,s^{-1}$ (4) (A) and master curve (reference strain rate is $1.7\times10^{-5}\,s^{-1}$) (B). The numbers of the samples correspond to the numbers in Table I.

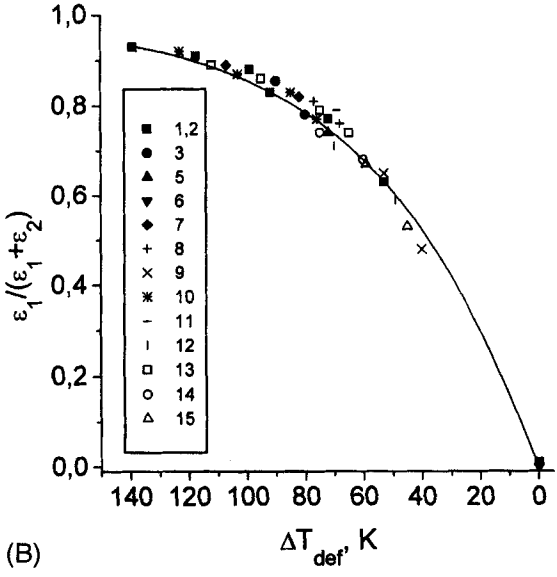

FIGURE 3 (Continued).

high-temperature component, and $\varepsilon_1/(\varepsilon_1+\varepsilon_2)$ tends to zero. At each ΔT_{def}, as strain rate is increased, $\varepsilon_1/(\varepsilon_1+\varepsilon_2)$ increases. The same effect of the strain rate and ΔT_{def} on $\varepsilon_1/(\varepsilon_1+\varepsilon_2)$ is described as a single master curve (Fig. 3(B)). This curve was obtained from Figure 3 (A) when curve 4 is fixed and curves 1 – 3 are shifted parallel to the ΔT_{def} axis.

Earlier [1 – 5], we discussed the physical and mechanical behavior of glassy polymers within the framework of the structural model which treats the structure of polymer glasses as a set of structural sublevels with different packing densities. According to this structural model, deformation of glassy polymers proceeds *via* a liquid-like local segmental mobility in the above structural sublevels.

This mechanism involves rotational and translational transitions of segments from initial state with minimum of energy (energy well) to adjacent energy well, that is, segmental relaxation similar to that in rubber. These transitions are associated with the *trans-gauche* conformational changes and require the overcoming of the potential barrier through intermediate high-energy excited states. Obviously, within the certain structural sublevels, the occurrence of these microscopic events is controlled by local packing density.

The onset of shear deformation in glassy polymer is provided by the stress-activated segmental mobility localized in the structural sublevels with lowered packing densities. With increasing strain, the propagation of shear bands and the development of resultant macroscopic deformation are controlled by a gradual stress activation of segmental mobility in the structural sublevels with increased packing densities. At yield point, the segments in all structural sublevels are involved in the stress activation and relaxation. Further post-yield (steady-state) deformation is associated with the increasing of sample volume incorporated in shear bands while the stress activation of new microscopic structural sublevels is not observed.

In connection with this, at each stage of the post-yield deformation, the deformed polymer is likely to be characterized by a set of high-energy stress-activated segments and low-energy relaxed segments. Under unloading and heating, the thermal activation of the segmental mobility is responsible for the macroscopic recovery of residual deformation *via* the transition of the above segments to their original states.

For high-energy excited segments, backward motion to the original states proceeds easily even at temperatures below T_g. As the temperature is increased, these segments become involved in the thermal activation in the structural sublevels with increased packing densities, and this trend contributes to the low-temperature component of the temperature-induced recovery of residual deformation. For the low-energy segments, which relaxed during loading, rubber-like transition to their initial state takes place only at T_g when co-operative segmental mobility is activated in the whole polymer sample, and glass-rubber transition occurs. This mode of segmental mobility is responsible the high-temperature component of the recovery of residual deformation. From this standpoint, for the deformed polymer samples, the ratio between low-temperature and high-temperature components of the temperature-induced recovery of residual deformation describes the ratio between the high-energy excited and low-energy relaxed segments and provides an important information concerning the time- and temperature-dependent mechanical behavior of glassy polymers.

Decreasing ΔT_{def} is accompanied by the enhancement of segmental relaxation in local structural sublevels during deformation and, as a result, by the decreasing $\varepsilon_1/(\varepsilon_1 + \varepsilon_2)$. At constant ΔT_{def}, as strain rate

is increased, segments in the local structural sublevels have no sufficient time to relax, and deformed polymer sample is enriched with the high-energy excited segments. As a result, with increasing the strain rate $\varepsilon_1/(\varepsilon_1+\varepsilon_2)$ increases. Note that the dynamics of segmental mobility has a well-pronounced effect on the mechanical properties of polymer glasses. For all polymer samples studied in this work, both elastic modulus and yield stress correlate well with $\varepsilon_1/(\varepsilon_1+\varepsilon_2)$ (Fig. 4).

Hence, parameter $\varepsilon_1/(\varepsilon_1+\varepsilon_2)$ may be treated as a universal physical parameter which describes the physical and mechanical behavior of polymer glasses independently of their chemical structure and composition. This parameter stands for the macroscopic manifestation of the microscopic local segmental mobility, which is responsible for the development of deformation and depends on ΔT_{def}. From the structural viewpoint, the influence of ΔT_{def} on the dynamics of segmental mobility may be attributed to the influence of ΔT_{def} on the initial state of polymer structure, primarily, on the content of free volume.

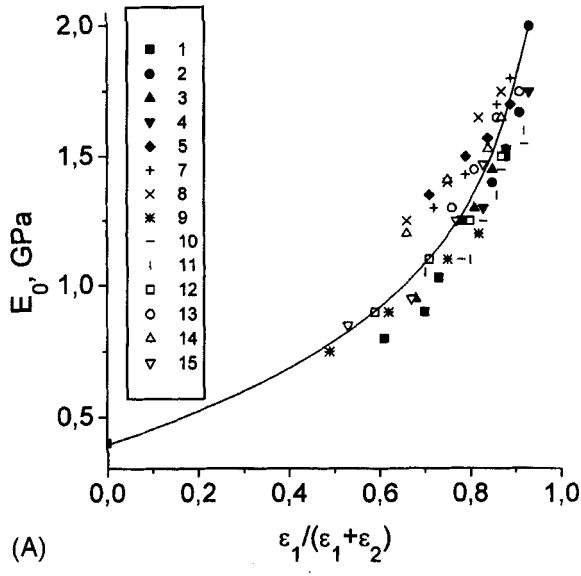

FIGURE 4 Elastic modulus E_0 (A) and yield stress σ_y (B) *versus* contribution from the low-temperature component to the total recovery of residual deformation $\varepsilon_1/(\varepsilon_1+\varepsilon_2)$. The numbers of the samples correspond to the numbers in Table I.

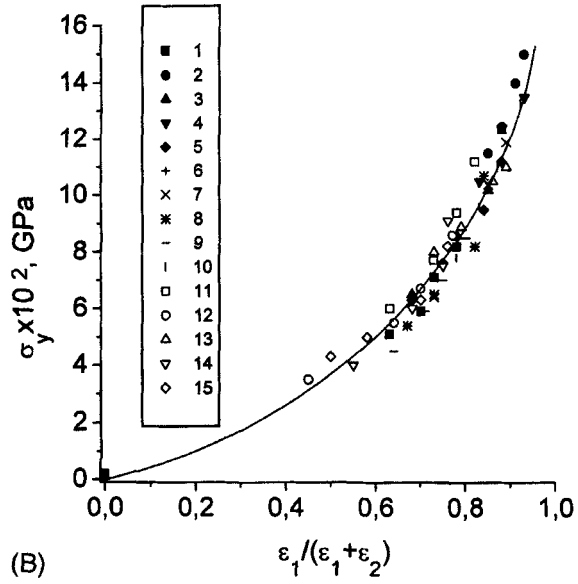

FIGURE 4 (Continued).

To verify this assumption, PALS was used to identify the changes in the free volume content as induced by copolymerization of methyl methacrylate with various methacrylic monomers. For initial PMMA and MMA copolymers, the PAL characteristics of the three-component analysis are listed in Table II.

As follows from Table II, the copolymerization of MMA with OMA and LMA is accompanied by a certain increase in annihilation parameters of the longest-lived component (τ_3 and I_3), whereas annihilation parameters of shorter-lived component (τ_2 and I_2) show no noticeable changes. Increasing annihilation characteristics of the third component of the PAL spectra is associated with the increasing free volume content in copolymer samples, primarily, in the structural sublevels with lowered packing densities. Taking into account the fact that as a result of copolymerization T_g decreases (Tab. I), one may anticipate that free volume content increases when T_g approaches the testing temperature of the PAL measurements (293 K).

For PMMA, the effect of temperature on the annihilation parameters was studied in [39] at temperatures varying from 83 to 523 K. For the four-component analysis, the annihilation parameters of the

longest-lived component (τ_4 and I_4) were shown to increase with increasing temperature. For testing temperatures at which deformation of PMMA was carried out (Tab. I), the corresponding annihilation parameters are listed in Table III. The annihilation parameters of the third component (τ_3 and I_3) remain unchanged and lie in the range of 0.9 ± 0.1 ns and $8 \pm 1\%$, respectively. For the annihilation parameters

TABLE II Annihilation parameters of PMMA and copolymer samples for the three-component analysis of positron lifetime spectra from the PATFIT (test temperature, 293 K)

Sample	τ_1, *ns*	I_1, %	τ_2, *ns*	I_2, %	τ_3, *ns*	I_3, %
PMMA	0.227 ±0.05	37.25 ±1.04	0.452 fixed	30.31 ±2.67	1.930 ±0.01	24.87 ±0.21
	0.240 ±0.003	44.23 ±1.29	0.482 ±0.008	31.48 ±1.21	1.962 ±0.005	24.29 ±0.11
PMMA with						
0.1 wt%	0.240 ±0.003	44.24 ±1.29	0.480 ±0.008	31.40 ±0.005	1.960 ±0.005	24.32 ±0.11
0.5 wt%	0.242 ±0.003	44.11 ±1.11	0.478 ±0.008	31.24 ±1.05	1.970 ±0.005	24.78 ±0.1
1.3 wt%	0.234 ±0.003	44.09 ±1.08	0.484 ±0.007	31.09 ±1.01	1.981 ±0.004	24.83 ±0.1
of DES (MMA -*co*- OMA) 95/5	0.238 ±0.04	42.42 ±0.84	0.466 fixed	31.92 ±0.96	2.030 ±0.01	25.60 ±0.16
(MMA -*co*- OMA) 80/20	0.237 ±0.04	43.39 ±0.80	0.476 fixed	30.34 ±0.90	2.240 ±0.01	26.50 ±0.15
(MMA -*co*- LMA) 85/15	0.229 ±0.04	41.92 ±0.80	0.476 fixed	31.44 ±0.90	2.28 ±0.01	26.8 ±0.16

TABLE III Annihilation parameters of the longest-lived component of PMMA for four-component analysis of positron lifetime spectra [39]

Test temperature, K	τ_4, *ns*	I_4, %
293	2.01	24.8
320	2.09	26.3
333	2.11	26.9
353	2.17	27.7

of the second component, τ_2 slightly increases. In other words, for PMMA, when testing temperatures approach T_g, an increase in the annihilation parameters of the fourth component of PAL spectra suggests an increase in the free volume content in the polymer samples.

Hence, the PAL measurements show that the free volume content in the polymer samples increases as the temperature interval between testing temperature and T_g is decreased by increasing the testing temperature at a fixed T_g (PMMA) or by decreasing T_g at a fixed testing temperature (MMA copolymers). Note that these speculations are based on the examination of the annihilation parameters of the third component (this work) and annihilation parameters of the fourth component [39]. The annihilation parameters of the third component [39] were ignored even though lifetime $\tau_3 = 0.9 \pm 0.1$ ns is long enough to be associated with ortho-positronium pick-off annihilation. To justify this situation, for two samples – PMMA and copolymer MMA/OMA (80/20), additional measurements with higher statistics (1.5×10^7 counts) were carried out. The results were treated in terms of the four-component PATFIT program. As compared with the POSGAUSS program [39], preliminary measured resolution function (FWHM = 230 ps) was used. Later on, two approaches were used: unconstrained four-component analysis (i) and constrained four-component analysis (ii). The second approach was similar to that used in [39] with $I_1 = (I_3 + I_4)/3$ and specific time of singlet positronium $\tau_1 = {}^s\tau_0 = 0.125$ ns.

Note that the first approach seems to be more advantageous (Tab. IV). In the case of the unconstrained four-component analysis, parameter χ^2/ν is much lower than that used in the constrained analysis.

As shown by unconstrained analysis, the value of $I_3 + I_4$ is about the same as I_3 in the three-component analysis (Tabs. II and IV). On the other hand, this value (Tab. IV) is comparable with I_4 (Tab. III) and much lower than $I_3 + I_4$ as obtained in [39]. For PMMA at 293 K, lifetime $\tau_3 = 1.46 \pm 0.21$ ns was estimated using the unconstrained four-component analysis (Tab. IV), and this value is much higher than $\tau_3 = 0.9 \pm 0.1$ ns as was estimated in [39].

The reason of this discrepancy is associated with a complicated character of PAL spectra of the test polymer samples. Singlet positronium lifetime partially overlaps the lifetimes of free non-localized positrons, which should be involved in the first component in

TABLE IV Annihilation parameters of PMMA and copolymer of MMA/OMA (80/20) for four-component analysis of positron lifetime spectra (test temperature, 293 K). The constraint: $I_1 = (I_3 + I_4)/3$, $\tau_1 = {}^s\tau_0$

Sample	*Approach*	τ_1, ns	$I_1, \%$	τ_2, ns	$I_2, \%$	τ_3, ns	$I_3, \%$	τ_4, ns	$I_4, \%$	χ^2/ν
PMMA	Unconstrained	0.194 ±0.007	27.06 ±2.33	0.393 ±0.010	46.18 ±1.91	1.46 ±0.21	10.38 ±4.74	2.13 ±0.10	16.37 ±5.20	1.089
	Constrained	0.125 (fixed)	10.87 ±0.12	0.323 ±0.001	56.54 ±0.49	0.80 ±0.03	9.65 ±0.26	2.00 ±0.01	22.94 ±0.28	1.252
(MMA -*co*- OMA)	Unconstrained	0.191 ±0.006	26.46 ±1.86	0.388 ±0.008	44.94 ±1.59	1.56 ±0.14	9.79 ±2.11	2.47 ±0.06	18.81 ±2.39	1.132
80/20	Constrained	0.125 (fixed)	11.06 ±0.08	0.322 ±0.001	55.74 ±0.33	0.90 ±0.03	8.88 ±0.17	2.33 ±0.01	24.31 ±0.22	1.399

the four-component analysis. The annihilation of the localized positrons is associated with the second component. In [39], as a result of artificial decrease in I_1 by the constraint and by fixing τ_1, a certain fraction of non-localized positrons is associated with I_2 [for constrained analysis, τ_2 is shown to be shorter than the corresponding value for unconstrained analysis (Tab. IV)]. Moreover, a certain fraction of the localized positrons contributes to I_3 [τ_3 in [39] is shorter than the corresponding value for unconstrained analysis (Tab. IV)]. Hence, in the case of the constrained analysis [39], the major fraction of the pick-off annihilation of triplet positronium is involved in the fourth (the longest-lived) component of the four-component analysis. These speculations allow one to conclude that the ortho-positronium annihilation in the test polymer samples is presented by the following parameters:

1. I_3 in the three-component unconstrained analysis (this work);
2. I_4 in the four-component constrained analysis [39];
3. $I_3 + I_4$ in the four-component unconstrained analysis (this work).

These results allowed us to establish the correlation between the values of the longest-lived components obtained in this work and in [39]. For PMMA deformed at different temperatures and for MMA copolymers, Figure 5 shows the effect of $T_g - T_{\text{test}}$ on the annihilation parameters such as lifetime τ_L and intensity I_L of the longest-lived components (in our case, the third component and the fourth component in [39]) (Tabs. III and IV). An increase in the intensity I_L and lifetime τ_L of the longest-lived annihilation component implies an adequate increase in free volume as a result of reducing $T_g - T_{\text{test}}$ temperature interval *via* increasing testing temperature and copolymerization. Increasing free volume in polymer samples is responsible for the enhancement of segmental relaxation and resulting decrease in both σ_y and $\varepsilon_1/(\varepsilon_1 + \varepsilon_2)$ (Fig. 6).

Note that, for PMMA containing DES, the mechanical and PAL data also agree with the above dependences (Fig. 6), even though DES has no effect on T_g of PMMA and on the temperature interval between T_g and T_{def} (Tab. I). This behavior was formalized [40] in terms of the structural plasticization of polymers.

A poor compatibility of DES and PMMA prevents a uniform distribution of DES in polymer, and no effect of DES on T_g of PMMA

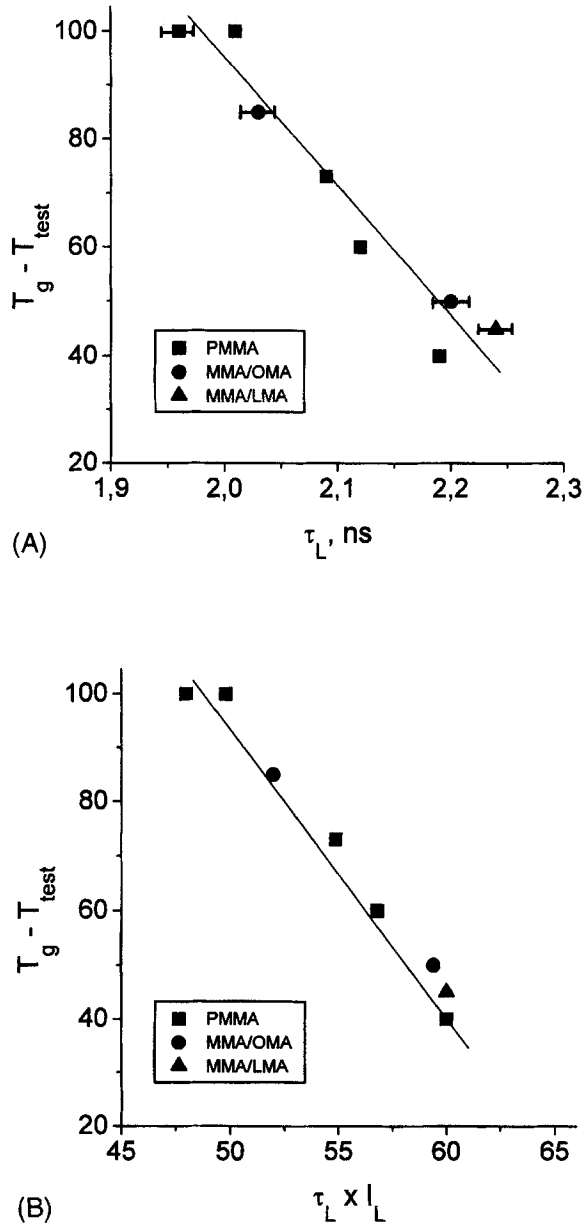

FIGURE 5 The difference between glass transition temperature and testing temperature $T_g - T_{test}$ *versus* lifetime τ_L of the longest-lived components (A) and product of the lifetime τ_L and intensity I_L (B) of the PAL spectra for PMMA and MMA copolymers.

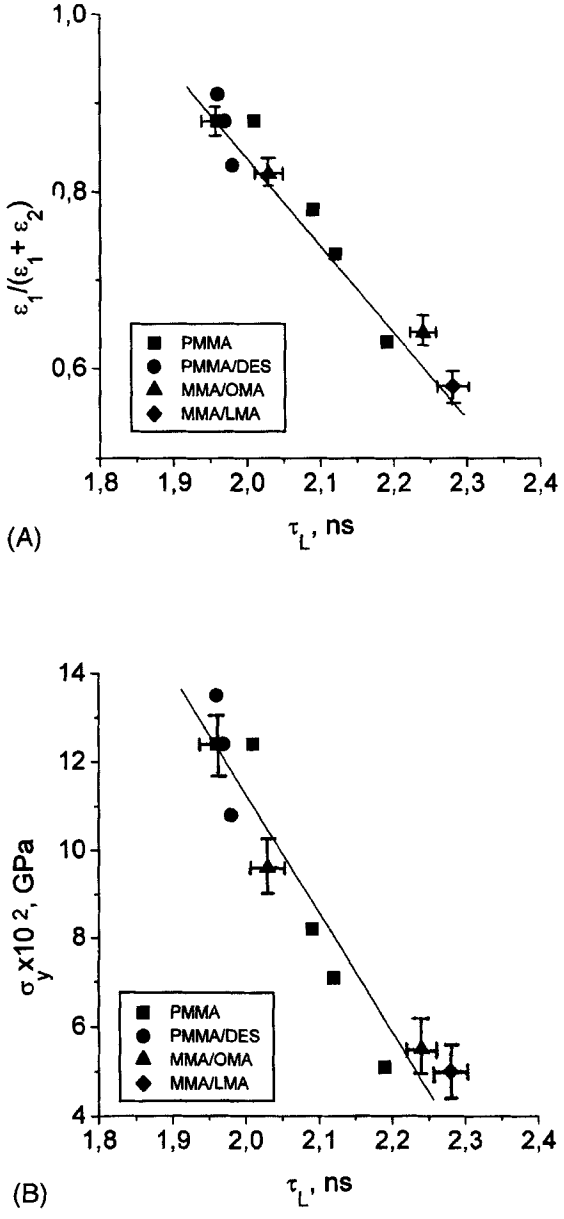

FIGURE 6 Contribution from the low-temperature component to the relaxation of residual deformation $\varepsilon_1/(\varepsilon_1+\varepsilon_2)$ (A) and yield stress σ_y (B) *versus* lifetime τ_L of the longest-lived components of the PAL spectra, and contribution the from low-temperature component to the relaxation of residual deformation $\varepsilon_1/(\varepsilon_1+\varepsilon_2)$ (C) and yield stress σ_y (D) *versus* the product of lifetime τ_L and intensity I_L of the longest-lived components of the PAL spectra for PMMA and MMA copolymers.

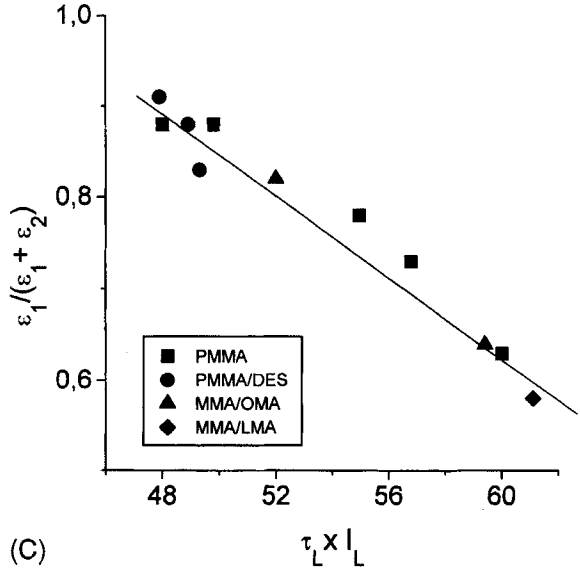

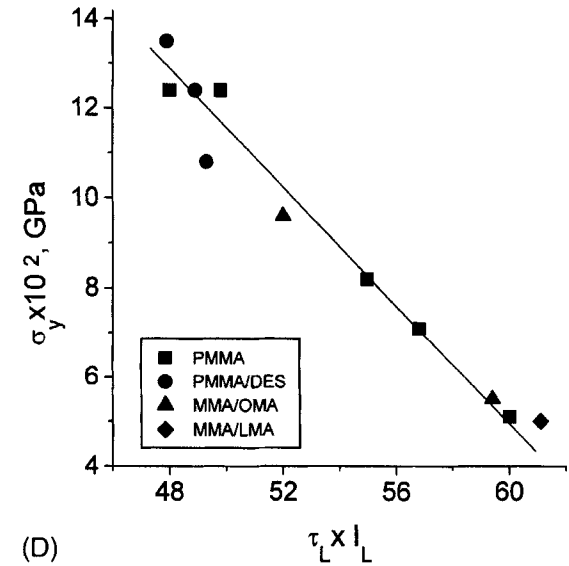

FIGURE 6 (Continued).

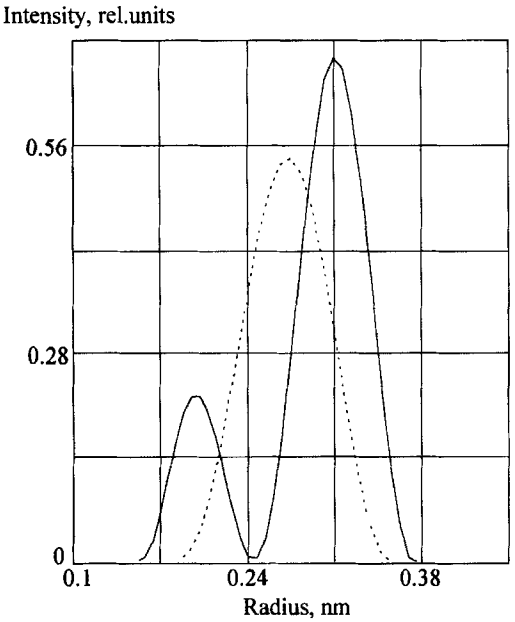

FIGURE 7 Probability density function $f(R)$ of positron annihilation in the free volume holes with radius R. PMMA – dashed line, copolymer MMA/OMA (80/20) – solid line.

is observed. However, the introduction of DES to PMMA changes the mechanical characteristics of polymer such as E_0, σ_y and $\varepsilon_1/(\varepsilon_1+\varepsilon_2)$ (Tab. I).

At low concentration of DES (0.1 wt%) in the feed mixture with MMA, during polymerization, DES molecules are pushed out to the large free volume microholes within the structural sublevels with lowered packing densities. As a result, in these structural sublevels, segmental mobility is inhibited, and both σ_y and $\varepsilon_1/(\varepsilon_1+\varepsilon_2)$ increase (Tab. I). In this case, the annihilation parameters of the PMMA/DES samples are comparable to those of initial PMMA (Tab. II), that is, DES has no marked influence on the free volume in PMMA (Fig. 7).

As the concentration of DES in MMA increases to 0.5 and 1.3 wt%, during polymerization, DES molecules prevent close packaging of the growing PMMA macrochains. As a result, in the final polymer samples free volume increases [I_3 and τ_3 increase (Tab. II)], and E_0, σ_y, and $\varepsilon_1/(\varepsilon_1+\varepsilon_2)$ decrease (Tab. I).

Hence, the combination of the PALS with mechanical tests allows one to conclude that mechanical properties of glassy polymers correlate with the free volume content independently of its variations: either by changing testing temperature, or copolymerization, or plasticization.

Finally, let us discuss the results of the continuos analysis of the PAL spectra for PMMA and MMA/OMA (80/20) copolymer samples using CONTIN program [35–38]. The advantages of this program are associated with the fact that, in this case, there is no need to fix the number of the components. This program provides a continuous size distribution of the elementary free volumes where positronium is localized. For these samples, Figure 5 shows a continuous size distribution of the elementary free volumes $f(R)$ obtained by a standard procedure [36] (75 points in the solution and Si single-crystalline reference sample with a single lifetime of 220 ps) from the long-lived positronium portions of the PAL spectra.

Note that, according to the PATFIT four-component analysis, for the MMA/OMA copolymer sample, CONTIN program reveals two peaks of size distribution of free volume holes with radius of 0.2 and 0.31 nm, respectively (Fig. 6, solid line). Only one peak of this distribution is resolved for PMMA (Fig. 6, dashed line). This fact may be explained by larger uncertainties in the estimation of I_3 and I_4 for PMMA samples in the PATFIT analysis as compared with those for MMA/OMA sample (Tab. IV). For these two samples, the CONTIN analysis shows no difference between the intensities of the positronium components (28.7% of total spectrum), and the corresponding dimensions of free volume microregions in MMA/OMA sample appear to be much higher.

CONCLUSION

For various glassy polymers, the ratio between the low-temperature and high-temperature components of the temperature-induced recovery of residual deformation was treated as a universal physical parameter. This parameter describes the development of the deformation and mechanical behavior of polymer glasses independently of their chemical structure. This ratio is controlled by the relative deformation temperature ΔT_{def}, that is, the difference between T_g and

T_{def}. A universal character of this phenomenon is associated with the general molecular mechanism of the deformation of glassy polymers. This mechanism is based on gradual activation of the local segmental mobility within the certain structural sublevels. As ΔT_{def} is decreased, both local segmental mobility and relaxation during deformation are enhanced. As a result, the low-temperature (at temperatures below T_g) recoverability of residual deformation and mechanical properties such as elastic modulus and yield stress decrease.

The PAL measurements show that the dynamics of the local segmental mobility and resultant mechanical behavior of glassy polymers are controlled only by the development of an adequate free volume content at each ΔT_{def}. This trend is independent of the variations in ΔT_{def}, either by varying the testing temperature or by physicochemical modification (plasticization or copolymerization).

For glassy polymers, the combination of mechanical tests with the PALS allowed one to establish a general correlation between the microstructural state, microscopic molecular (segmental) mobility, and resultant macroscopic mechanical response.

Acknowledgement

We would like to thank Dr. D. V. Trachenko for the preparation of the test copolymer samples. This work was supported by the Russian Foundation of Basic Researches; project No. 98-03-32859.

References

[1] Arzhakov, S. A., Bakeev, N. F. and Kabanov, V. A. (1973). *Vysokomol. Soedin.*, **A13**, 1154 (in Russian).
[2] Arzhakov, S. A. (1975). *Doctorate (Chem.) Dissertation*, Moscow: Karpov Institute of Physical Chemistry, (in Russian).
[3] Arzhakov, M. S., Arzhakov, S. A. and Chernavin, V. A. (1996). *New Polymeric Mater.*, **5**, 43.
[4] Arzhakov, M. S. and Arzhakov, S. A. (1997). *Proc. 10th Intern. Conf. on Deformation*, Yield and Fracture of Polymers, Cambridge, p. 72.
[5] Arzhakov, M. S., Arzhakov, S. A. and Zaikov, G. E., Eds. (1997). Structural and Mechanical Behavior of Glassy Polymers, Commack, New York: Nova Science Publ.
[6] Oleinik, E. F., Salamatina, O. B., Rudnev, S. N. and Shenogin, S. V. (1993). *Polymer Science*, **35**, 1532.
[7] Oleinik, E. F., Salamatina, O. B., Rudnev, S. N. and Shenogin, S. V. (1995). *Polymers for Advanced Technologies*, **6**, 1.

[8] Diaz-Calleja, R., Perez, J., Gomez-Ribelles, J. L. and Ribes-Greus, A. (1989). *Makromol. Chem., Macromol. Symp.*, **27**, 289.
[9] Quinson, R., Perez, J., Germain, Y. and Murraciole, J. M. (1995). *Polymer*, **36**, 743.
[10] Gauthier, C., Perez, J., Oleinik, E., Rudnev, S., Slavetskaya, T., Kravchenko, M. and Salamatina, O. (1997). *Proc. 10th Intern. Conf. on Deformation*, Yield and Fracture of Polymers, Cambridge, p. 64.
[11] Atzuta, M. and Turner, D. T. (1982). *J. Mater. Sci., Lett.*, **1**, 167.
[12] Yeh, G. S. J. (1979). *Proc. IUPAC Macro 26th Symp.*, Maintz, **2**, 1176.
[13] Kelley, F. N. and Trainor, D. R. (1982). *Polym. Bull.*, **7**, 369.
[14] Geil, P. H. (1987). *Proc. 17th Intern. Symp.*, New York, London, p. 83.
[15] Wendorff, J. (1982). *Polymer*, **23**, 543.
[16] Arzhakov, M. S., Arzhakov, S. A., Gustov, V. V., Kevdina, I. B. and Shantarovich, V. P. (1998). *Intern. J. Polymeric Mater.*, **39**, 319.
[17] Tanio, N., Koike, Y. and Ohtsuka, Y. (1989). *Polym. J.*, **21**, 259.
[18] Kevdina, I. B., Arzhakov, M. S. and Shantarovich, V. P. (1995). *Polymer Science*, **B37**, 171.
[19] Goldanskii, A. V., Onischuk, V. A. and Shantarovich, V. P. (1987). *Phys. Status Solidi*, **A102**, 559.
[20] Sanchez, V., Lopez, R., Fucugauchi, L. A. and Ito, Y. (1995). *J. Appl. Polym. Sci.*, **56**, 779.
[21] Macquenn, R. C. and Granata, R. D. (1993). *J. Polym. Sci. Part B: Polym. Phys.*, **31**, 971.
[22] Wang, S. J., Wang, C. L. and Wang, B. (1996). *J. Radioanalytical and Nuclear Chem.*, **210**, 407.
[23] Hasan, O. A., Boyce, M. C., Li, X. S. and Berko, S. (1993). *J. Polym. Sci. Part B: Polym. Phys.*, **31**, 185.
[24] Boyce, M. C. (1997). *Proc. 10th Intern. Conf. on Deformation*, Yield and Fracture of Polymers, Cambridge, p. 63.
[25] Shantarovich, V. P. (1997). *Proc. 10th Intern. Conf. on Deformation*, Yield and Fracture of Polymers, Cambridge, p. 215.
[26] Ito, Y. (1995). *Mater. Sci. Forum*, **175–178**, 627.
[27] Ito, K., Ujihira, Y., Yamashita, T. and Horie, K. (1996). *J. Radioanalitical and Nuclear Chem.*, **210**, 505.
[28] Jean, Y. C. and Wang, Y. Y. (1989). *Positron Annihilation*, Singapore: World Scientific, p. 787.
[29] Brandt, W., Berko, S. and Walker, W. W. (1960). *Phys. Rev.*, **120**, 1289.
[30] Goldanskii, A. V., Onischuk, V. A. and Shantarovich, V. P. (1989). *Positron Annihilation*, Singapore: World Scientific, p. 778.
[31] Brandt, W. and Paulin, R. (1972). *Phys. Rev.*, **5**, 2430.
[32] Shantarovich, V. P. (1996). *J. Radioanalitycal and Nuclear Chem.*, **210**, 357.
[33] Shantarovich, V. P., Kleiner, B. I., Alent'ev, A. Yu., Kevdina, I. B., Azamatova, Z. K. and Filimonov, M. K. (1997). *Khim. Vys. Energ.*, **31**, 494 (in Russian).
[34] Kirkegaard, P., Pedersen, N. J. and Eldrup, M. (1989). *Prepr.* RISO-M-2740.
[35] Provencher, S. W. (1982). *Comp. Phys. Commun.*, **27**, 229.
[36] Nakanishi, M., Wang, S. J. and Jean, Y. C. (1988). In: *Positron Annihilation Study of Fluids*, Sharma, S. C., Ed., Singapore: World Scientific, p. 292.
[37] Gregory, R. B. (1991). *J. Appl. Phys.*, **70**, 4665.
[38] Deng, Q. and Jean, Y. C. (1993). *Macromolecules*, **26**, 30.
[39] Kindl, P. and Reiter, G. (1989). *Positron Annihilation*, Singapore: World Scientific, p. 806.
[40] Arzhakov, M. S., Arzhakov, S. A., Gustov, V. V., Kevdina, I. B. and Shantarovich, V. P. (1999). *Intern. J. Polymeric Mater.* (in press).